$NdFeO_3$ nanocrystals under glycine nitrate combustion formation

Ekaterina Tugova [a], Sergey Yastrebov [a], O.N. Karpov [a], Roger Smith [b]

[a] *A.F. Ioffe Physicotechnical Institute, St.Petersburg, Russia*

[b] *School of Science, Loughborough University, Loughborough, LE11 3TU, United Kingdom*

Abstract

Nanocrystalline perovskite $NdFeO_3$ with the orthorhombic structure was prepared by a glycine nitrate combustion method under different technological conditions. The starting materials $Fe(NO_3)_3 \cdot 9H_2O$, $Nd(NO_3)_3 \cdot 6H_2O$ in stoichiometric amounts and H_2NCH_2COOH were used. These quantities were varied by changing the ratio of glycine moles to metal nitrate moles (G/N) in the range between 0.25 to 0.75. The prepared $NdFeO_3$ nanocrystals were characterized by X-ray diffraction (XRD) and electron microscopy. Decomposition of the XRD diffraction profile using Voigt contours was exploited for analysis of the pattern in the area where the most prominent diffraction peak was situated. We demonstrate that Voigt functions reduce to Lorentzians for G/N=0.75 and 0.56. A volume-weighted diameter distribution function was derived using the width of the Lorentzians. The log-normal shape of the distribution is discussed in terms of the model, assuming exponential growth of cluster size in the time available for the $NdFeO_3$ nanograin to grow.

1 Introduction

The rare-earth orthoferrites, having perovskite structure of general formula $RFeO_3$ (where R is a rare-earth ion) [1,2] have attracted much interest due to their novel magnetic [3,4] and magneto-optic [4] properties and are still the subject of much research aimed at a better understanding of the properties of the magnetic subsystems and how interactions between them depend on external parameters, such as temperature, field, pressure, etc. [3,4]. Among them, $NdFeO_3$ is known to have an orthorhombically distorted perovskite structure [5]. This material represents itself as an ensemble of nanoclusters whose sizes are statistically distributed. It is well known that the size distribution

of the nanoclusters governs their magnetic energy which in turn controls the switching temperature of the superparamagnetic state of the ensemble. Thus the effect of the preparation conditions on the size distribution of the nanoclusters of rare earth perovskite is an important problem to be solved [6]. In this connection, the derivation of the size-distribution of nanoclusters from the experimental data (e.g. from X-ray diffraction data) is a key practical problem.

To this end we will exploit results of paper [7]. The authors of this paper presented an analysis which shows that the Lorentzian (Cauchy) shape of the X-ray diffraction contour results in a log-normal distribution for the nanoclusters' diameter. The link between the Lorentzian parameters and parameters for the log-normal distribution is also presented in paper [8]. In this paper we exploited this link for analysis of the distribution function of $NdFeO_3$ that emerged during combustion. This kind of distribution may be valid for the early stage of cluster formation, i.e. the nucleation stage. We will show that the log-normal distribution is relevant for the formation of nanoclusters of $NdFe2O_3$ when their nucleation occurs in the course of simultaneous combustion of glycine nitrate and nitrates of iron and neodymium, correspondingly. To show this we perform analysis of strongest diffraction peak by its decomposition by a set of Voigt functions (Voigtians) [8].

The Voigtian is a convolution of Gaussian and Lorentzian functions (sometimes termed Cauchy functions), that can distinguish between the contributions of lattice strain and nanocluster size to the overall X-ray diffraction line broadening [8]. This decomposition will be done here by a numerical fit. In this regard we select the strongest diffraction peak to diminish the influence of experimental noise to the fitting results. This procedure may be performed routinely to achieve criteria for the best fit to the experimental diffraction profile. In this model the Gaussian function detects the lattice strain and the Lorentzian shows the influence to the broadening caused by the log-normal size distribution of the spherical particles forming the ensemble.

2 Experimental

$NdFeO_3$ nanocrystals have been synthesized by a glycine-nitrate combustion method. As starting materials $Fe(NO_3)_3 \cdot 9H_2O$, $Nd(NO_3)_3 \cdot 6H_2O$ in stoichiometric amounts and H_2NCH_2COOH are used. The quantities are varied by changing a parameter G/N in the range between 0.25 to 0.75. This parameter was calculated using the following equation: $\frac{G}{N} = \frac{n_{Gly}}{n'_{NO_3}+n''_{NO_3}}$, where n_{Gly} is number of glycine moles n'_{NO_3} is number of moles for nitrate groups of iron nitrate and n''_{NO_3} is the number of moles of nitrate groups generated

from neodymium nitrate. The resulting precursor was placed into a stainless steel chamber and subsequently heated up to 250° C. The phase composition and sequence of the phase transformations of $NdFeO_3$ are characterized by powder X-ray diffraction (XRD) using a Shimadzu XRD-7000 instrument with monochromatic $CuK\alpha$ radiation with wavelength λ= 1.54186 $\mathring{A}$.

Scanning electron microscopy (SEM) images of the sample's surface are presented in Fig.1. One can see a porous pattern in the figure. The pores and fractal-like structures in the images show evidence of gas emission during combustion.

XRD patterns are presented in Fig.2 for various G/N ratios. All peaks are subscripted in terms of the crystal planes that produce the XRD pattern, as was done in paper [2]. There is a good coincidence in positions of the peaks presented in Fig.2 and elsewhere (e.g., see [2]). The shoulder that appears at about 32.5° in most of the diffraction patterns may be attributed to a contribution from nanoclusters in a new phase with slightly different lattice parameters from ones for $NdFeO_3$. The rest of the peaks are fingerprints signifying the presence of $NdFeO_3$ particles in the ashes, that is a substance formed as result of combustion. One may detect a slight variation of line shapes of the diffraction peaks with a change in the G/N ratio. To investigate this effect in some detail we enlarged the most intense peak, as is depicted in Fig.2, right column. One may see that three diffraction peaks contribute to the strongest peak. While all three peaks are well resolved for this substance for G/N ratio equal to 0.75 and 0.56, the peak for $G/N = 0.35$ occurs more smeared. In addition the overall number of Voigtians contributing to the strongest peak in this case reduced to two. Moreover, for G/N equal to 0.75 and 0.56 the Voigtians reduce to Lorentzians. This difference indicates that for the case $G/N = 0.35$ the lattice of the nanoclusters is strained.

3 Formalism

Authors of paper [7] have shown that for the case of log-normal distribution of nanoparticles of spherical shape, the resulting XRD profile follows the Lorentzian (Cauchy) law. Also there exists the following relation between the full peak width measured at the half height of the Lorentzian and the parameters of a log-normal distribution. The contribution to the intensity of the diffraction peak with number i, V_i, as a function of double diffraction angle θ may be written in the following way:

$$V_i(\theta) = \int_{-\infty}^{\infty} S_i(\theta) L_i(\theta - \theta' - \theta_{0i}) d\theta', \tag{1}$$

where θ_{0i} is the double Bragg angle, $S_i(\theta)$ is a statistical distribution function, $L_i(\theta)$ is the Lorentzian (Cauchy function):

$$L_i(\theta) = \frac{2A_i}{\pi}\frac{w_{Li}}{\theta^2 + w_{Li}^2}. \tag{2}$$

Here w_{Li} is the full width of the Lorentz contour measured at its half height, and A_i is a constant. The parameter w_{Li} is linked to Scherrer's equation for the volume averaged mean size of crystallite D_{Shi}:

$$D_{Shi} = \frac{K\lambda}{w_{Li}cos(\theta_{0i}/2)}, \tag{3}$$

where K is a dimensionless constant that approximately equals unity, $\theta_{0i}/2$ is the Bragg angle. Equation (1) transforms to a Voigtian (Voigt function) when the function $S_i(\theta)$ follows the normal distribution (Gaussian) law:

$$S_i(\theta) = \sqrt{\frac{b_i}{\pi}}e^{-\theta^2 b_i}, \tag{4}$$

where $b_i = \frac{4ln(2)}{w_{Gi}^2}$ and w_{G_i} is full width of the Gaussian contour measured at its half height.

Authors of paper [7] show a relation between the full width measured at the half height of the Lorentzian and the following parameters of the log-normal distribution:

$$m = \left(\frac{3}{4}\right)^6 \frac{1}{\pi\frac{w_L}{2}} \tag{5}$$

and

$$\omega = ln\left(\frac{16}{9}\right)^{\frac{1}{2}}, \tag{6}$$

where m and ω are the median and logarithmic standard deviation, correspondingly. The density function, in its turn, is given by the equation:

$$f_{LN}(D; m, \omega) = \frac{1}{D\omega(2\pi)^{\frac{1}{2}}}exp\left(-\frac{ln(\frac{D}{m})^2}{2\omega^2}\right), \tag{7}$$

while the arithmetic mean is

$$\langle D \rangle = m \cdot exp\left(\frac{\omega^2}{2}\right). \tag{8}$$

The variance is

$$\sigma^2 = \langle D \rangle^2 (exp(\omega^2) - 1). \tag{9}$$

Also the area-weighted mean is

The moments of the distribution are:

$$\langle D_A \rangle = m \cdot exp\left(\frac{5}{2}\omega^2\right), \tag{10}$$

where $\langle D_A \rangle$ is an area-weighted mean. For the volume-weighted mean $\langle D_V \rangle$ the moment is:

$$\langle D_V \rangle = m \cdot exp\left(\frac{7}{2}\omega^2\right). \tag{11}$$

4 The numerical fitting and estimation

Fig 2, right column shows the XRD pattern of the substance subjected for combustion showing a set of well-pronounced peaks implying the formation of $NdFeO_3$ nanoclusters in the remains. After a comparison with literature data [2] one may see a coincidence of the XRD peaks position and, because of this coincidence, one may draw the conclusion that the investigated substance contains $NdFeO_3$ nanoclusters. For a detailed investigation the strongest XRD peak, namely the (121) peak should be considered. The choice to analyse this peak was made because of a lesser influence of the experimental noise on its line shape. The experimental XRD data are presented in the area of the strongest peak for the three samples with different G/N ratios, namely 0.75, 0.56 and 0.35), from top to bottom of the figure.

Analysis of the XRD profile can be performed by decomposition of the diffraction profiles presented in Fig.2 (right column), using equations (1), (2) and (4) as follows, exploiting the equation:

$$V(\theta) = \sum_{i=1}^{i_m} V_i(\theta). \tag{12}$$

Here $V(\theta)$ is the normalised intensity of the X-rays. The number of terms in the sum was selected empirically (i_m=4 for G/N ratio 0.75, 0.56 and i_m=2 for 0.35).

It was found that the theory fits the experiment reasonably well when the contribution of the Gaussians to equation (12) was neglected for the cases of samples with the 0.75, 0.56 G/N ratio. The resulting four Lorentzians are presented in Fig.2. The fitting parameters are given in the caption to Figure 1. It is seen that the parameters w_{Li} almost coincide with each other with values of $\approx 0.2 - 0.3^{\circ}$. Moreover, the diffraction peaks marked in the Figure by numbers 1, 3, 4 show evidence for the formation of the crystalline phase $NdFeO_3$ because of the coincidence of the peak positions with literature [2]. The origin of the peak marked by 2 will be discussed below. It was also found that the sum of two Voigtians (equations (1), (2) and (4)) fits the X-ray profile for the case of the sample produced for G/N=0.35, as one may see in Fig.2. The best fit parameters are also collected in the figure's caption. It is also seen that Lorentzian parameter for the most intensive peak presented in the third image is approximately given by $w_{Li} = 0.2^{\circ}$.

To calculate the particle distribution, one may use a value of $w_{Li} = 0.2^{\circ}$ converting it to radians and substituting the result into equation (5)-(7). This distribution function is shown in Fig.3. Also, using equation (8)-(11), one may estimate the mean values for $< D >$, σ, $\langle D_A \rangle$ and for $\langle D_V \rangle$ of 74 $\mathring{A}$, 65 $\mathring{A}$, 239 $\mathring{A}$ and 426 $\mathring{A}$, correspondingly.

5 Discussion and Conclusions

Analysis of the strongest peak (121) allowed us to fit the experimental data by a sum of Lorentzians for the samples produced with $G/N = 0.56$ and 0.75. This shows an absence of strain on the lattice of clusters. For $G/N = 0.35$ the experimental data is fit by a sum of Voigtians. This implies cluster formation with a strained lattice. Analysis of the strongest XRD peak (121) showed a contribution from at least three peaks to the overall intensity in the actual range of the diffraction angles where (121) peak dominates. The additional peaks belonging to a lattice of $NdFeO_3$ are (200) and (002) and the structure shown in Fig.2 should resemble a triplet. However, analysis reveals a fourth peak marked in the Figure by number 2 which does not match any crystallographic plains of $NdFeO_3$. This unexpected peak could result from a splitting of the peak (121). It may appear alternatively because of the formation of another crystalline form with slightly different stoichiometric indices from $NdFeO_3$ or by unaxial lattice strain. Moreover, for the case of the lattice strain a Voigtian line shape broadening might be expected but that does not occur in this case.

As a criterion for the correctness of our procedures of estimation of the distribution function, we used a value of Scherrer's diameter of the crystallite (see equation (3)). It is known that Scherrer's estimation of crystallite size is based on the volume averaged mean value [8]. Thus a comparison of the values obtained from equations (3) and (11) should demonstrate the correctness of the estimation of the distribution. For the case $w_{Li} = 0.2°$, Scherrer's diameter is approximately equal to $D_{Sh} \approx 420 - 430\mathring{A}$ (index i is omitted). Thus, the equality between D_{Sh} and $\langle D_V \rangle$ gives evidence for the correctness of our estimation of the distribution function.

During the analysis we used a model of spheres distributed according to a log-normal law which provides a good fit to the experimental data. This implies that the clusters that form in the course of combustion are spherical. Thus, we have to explain both how spherical clusters might be formed and how the conditions for the log normal distribution appear. First, the existence of pores must be postulated in the substance subjecting to a combustion, to establish the model. The porous matrix itself may be formed during the early stages of combustion by exhaust of gases, as Fig.1 shows and the clusters might be formed inside the pores. The spherical shape of the clusters may be explained in terms of an initial formation of a two-dimensional liquid phase followed by nanocluster nucleation, solidification and further growth. Actually, it is known from the literature that the temperature during glycine nitrate combustion may attain $2000K$, which is slightly less than the melting temperature of bulk $NdFeO_3$ (2068 K). At first sight, the ambient temperature of $2000K$ is not enough to melt the$NdFeO_3$ substance but the melting temperature, in its turn, decreases with a decreasing dimensionality of the layer containing $NdFeO_3$. Following paper [10], for a two-dimensional layer, the temperature drops down by a factor of 0.65: $T_{2D} = 0.65T_{3D}$. This two-dimensional phase may appear just after adsorption of gas precursors of $NdFeO_3$ by the internal surface of pore.

Once adsorbed by the surface, precursors may form a two-dimensional layer of $NdFeO_3$ that swiftly transforms to liquid, because the temperature inside the pore may exceed the melting point for two-dimensional $NdFeO_3$. Just after contact with the pore surface, melting liquid may transform to a spherical drop by wetting forces. The drop is now no longer two-dimensional and therefore the melting temperature could rise which causes crystallisation of the drop. Thus a reducing temperature with a lowering of dimensionality of the liquid may play an important role in $NdFeO_3$ cluster nucleation providing a mechanism for the formation of $NdFeO_3$ nanoclusters during the combustion. The further growth of nanograins localised in pores is controlled mainly by the subsequent adsorption of precursors and their diffusion along grain boundaries, bearing in mind a relatively high temperature of combustion that produces a high value of the diffusion coefficient in accordance with the Arrhenius law.

In probability theory, a log-normal distribution is a continuous probability distribution of a random variable whose logarithm is normally distributed. Thus if the random variable $\beta\tau = ln(D)$ is normally distributed, then the variable lnD has a lognormal distribution. Here β is a coefficient, and τ is the time available for a particle to grow in a pore. The exponential dependence between τ and D follows from the fundamental law of exponential population growth in the early stage of its formation [11].

Thus, a model of the log-normal distribution allowed us to fit XRD patterns of nanoclusters of$NdFeO_3$ produced by the combustion of glycine nitrate with metal nitrate precursors. The formation of spherical $NdFeO_3$ particles was explained in terms of the formation of a two-dimensional liquid altering its geometry after contact with the pore surface. The subsequent growth of the nanograin is controlled by a surface diffusion mechanism. The origin of the log-normal distribution follows the fundamental principles of growth of size of a population of atoms embedded in the cluster during the early stage of its formation.

6 Acknowledgements

The study was financially supported by the Russian Science Foundation (project no. 16-13-10252).

References

[1] Tugova E.A., Karpov O.N. Nanocrystalline perovskite-like oxides formation in Ln2O3 - Fe2O3 - H2O (Ln = La, Gd) systems // Nanosystems: physics, chemistry, mathematics. 2014. V. 5, 6. - P. 854-860.

[2] Mostafa Yousefi, Samaneh Soradi Zeid and Mozhgan Khorasani-Motlagh Synthesis and characterization of nano-structured perovskite type neodymium orthoferrite NdFeO3 Current Chemistry Letters 6 (2017) 23-30

[3] Kimel A. V., Kirilyuk A., Usachev P. A., Pisarev R. V., Balbashov A. M., and Rasing T. (2005) Ultrafast non-thermal control of magnetization by instantaneous photomagnetic pulses. Nature, 435 (7042) 655-657.

[4] Iida R., Satoh T., Shimura T., Kuroda K., Ivanov B. A., Tokunaga Y., and Tokura Y. (2011) Spectral dependence of photoinduced spin precession in DyFeO3. Phys. Rev. B, 84 (6) 064402.

[5] Przeniosło R., Sosnowska I., Loewenhaupt M., and Taylor A. (1995) Crystal field excitations of $NdFeO_3$. J. Magn. Magn. Mater., 140, 2151-2152.

[6] Popkov V.I., Almjasheva O.V., Panchuk V.V., Semenov V.G., Gusarov V.V. The Role of Pre-Nucleus States in Formation of Nanocrystalline Yttrium Orthoferrite // Doklady Chemistry. 2016. V.471, Part. 2, P.356-359.] (10.1134/S0012500816120041)

[7] T. Ida, S. Shimazaki, H. Hibino, H. Toraya Diffraction peak profiles from spherical crystallites with lognormal size distribution J. Appl. Cryst. (2003). 36, 1107-1115

[8] A. Siklitskaya, S. G. Yastrebov, R. Smith An interpretation of the strongest X-ray diffraction peak for various carbon nanoclusters Nanosystems: physics, chemistry, mathematics, 2016, 7 (2), P. 340–348

[9] Nanostructured materials. Selected synthesis methods, properties and applications., eds Ph.Knauth, J.Schoonman, Kluwer 2002, P.131 (183 P.)

[10] V.V. Gusarov The thermal effect of melting in polycrystalline systems Thermochimica Acta 256 (1995) 467-472

[11] Verhulst, Pierre-Francois (1845). "Recherches mathematiques sur la loi d'accroissement de la population" [Mathematical Researches into the Law of Population Growth Increase]. Nouveaux Memoires de l'Academie Royale des Sciences et Belles-Lettres de Bruxelles. 18: 142. Retrieved 2013-02-18.

7 Figure captions

Fig.1 SEM image of substance appeared after combustion of glycine nitrate and nitrates of metallic precursors of $NdFeO_3$ substance, for different G/N ratio.

Fig.2 Diffractograms of $NdFeO_3$ substance. Open circles stand for the experimental data and continous lines presen of result of best the fit. Data from top to bottom plotted for G/N ratio 0.75, 0.56 and 0.35 correspondingly. Left coumn. The diffraction patterns of substance appeared after combustion of glycine nitrate and nitrates of metallic precursors of $NdFeO_3$ substance, for different G/N ratio. Right coloumn. The diffractogramm detected in area where the most intensive diffraction peak for $NdFeO_3$ becomes dominant. The fitting parameters are collected correspondingly for the most intensive diffraction peak (left column), from top to bottom as follows; $\theta_{01} = 32.01 \pm 0.01^o$, $w_{L1} = 0.341 \pm 0.019^o$, $A_1 = 755 \pm 48$ arb. units, $\theta_{02} = 32.36 \pm 0.01^o$, $w_{L2} = 0.221 \pm 0.018^o$, $A_2 = 784 \pm 100$ arb. units; $\theta_{03} = 32.53 \pm 0.002^o$, $w_{L3} = 0.223 \pm 0.005^o$, $A_3 = 2494 \pm 93$ arb. units; $\theta_{04} = 32.84 \pm 0.003^o$, $w_{L4} = 0.15 \pm 0.01^o$, $A_3 = 306 \pm 20$ arb. units; $\theta_{01} = 32.07 \pm 0.01^o$, $w_{L1} = 0.26 \pm 0.03^o$, $A_1 = 399 \pm 68$ arb. units, $\theta_{02} = 32.39 \pm 0.01^o$, $w_{L2} = 0.29 \pm 0.04^o$, $A_2 = 1085 \pm 199$ arb. units; $\theta_{03} = 32.58 \pm 0.002^o$, $w_{L3} = 0.212 \pm 0.007^o$, $A_3 = 2141 \pm 138$ arb. units; $\theta_{04} = 32.88 \pm 0.004^o$, $w_{L4} = 0.11 \pm 0.01^o$, $A_3 = 176 \pm 17$ arb. units; $\theta_{02} = 32.50 \pm 0.006^o$, $A_2 = 2858 \pm 59$ arb. units, $w_{L2} = 0.20 \pm 0.02^o$, $w_{G2} = 0.39 \pm 0.03^o$, $\theta_{01} = 32.04 \pm 0.008^o$, $A_1 = 215 \pm 40$ arb. units $w_{L1} = 0.0.059 \pm 0.2^o$, $w_{G1} = 0.38 \pm 0.13^o$.

Fig.3 Typical distribution of number of particles distribution function of $NdFeO_3$ nanoclusters vs their diameter (calculated using equations (5)-(7) for $w_L = 0.2^o$.

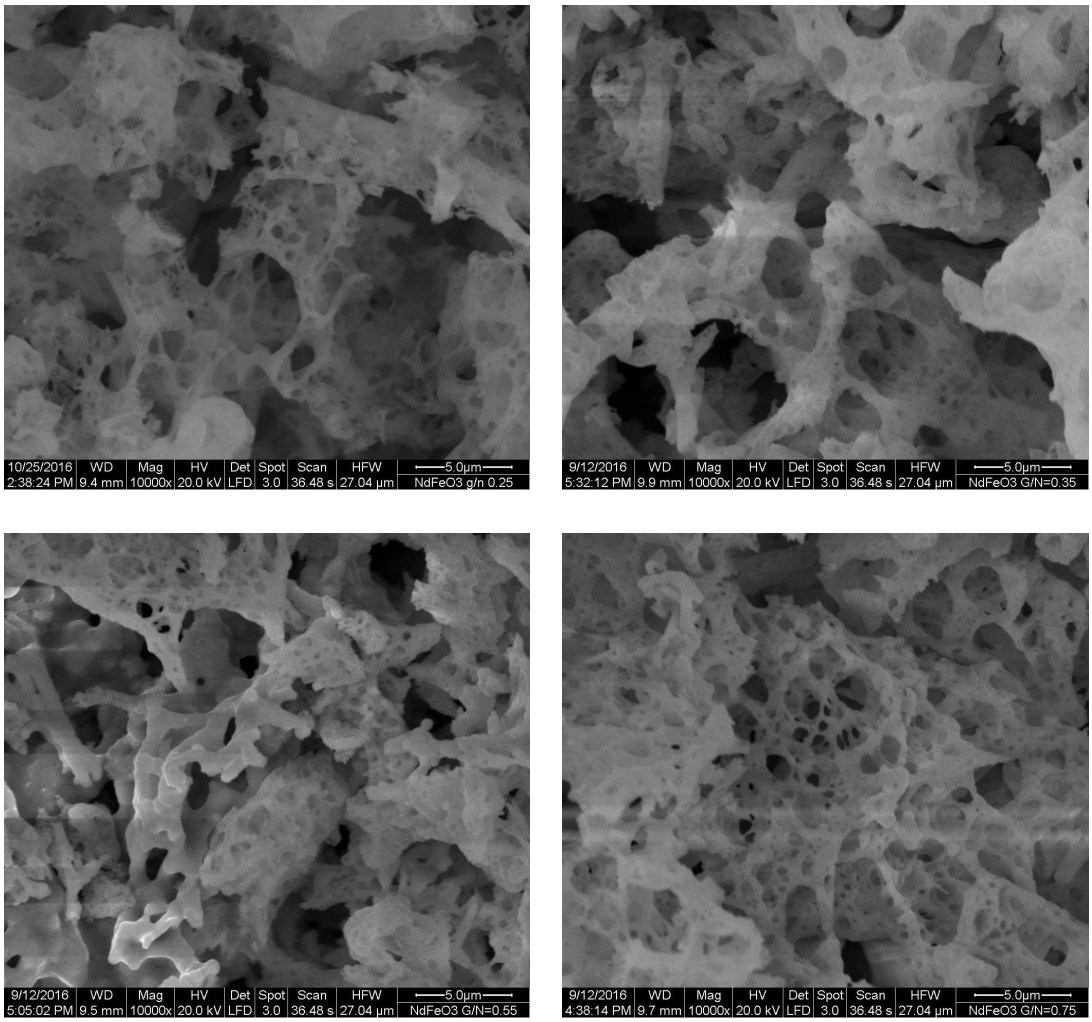
10/25/2016 WD Mag HV Det Spot Scan HFW 5.0µm
2:38:24 PM 9.4 mm 10000x 20.0 kV LFD 3.0 36.48 s 27.04 µm NdFeO3 g/n 0.25
9/12/2016 WD Mag HV Det Spot Scan HFW 5.0µm
5:32:12 PM 9.9 mm 10000x 20.0 kV LFD 3.0 36.48 s 27.04 µm NdFeO3 G/N=0.35
9/12/2016 WD Mag HV Det Spot Scan HFW 5.0µm
5:05:02 PM 9.5 mm 10000x 20.0 kV LFD 3.0 36.48 s 27.04 µm NdFeO3 G/N=0.55
9/12/2016 WD Mag HV Det Spot Scan HFW 5.0µm
4:38:14 PM 9.7 mm 10000x 20.0 kV LFD 3.0 36.48 s 27.04 µm NdFeO3 G/N=0.75

Fig. 1.

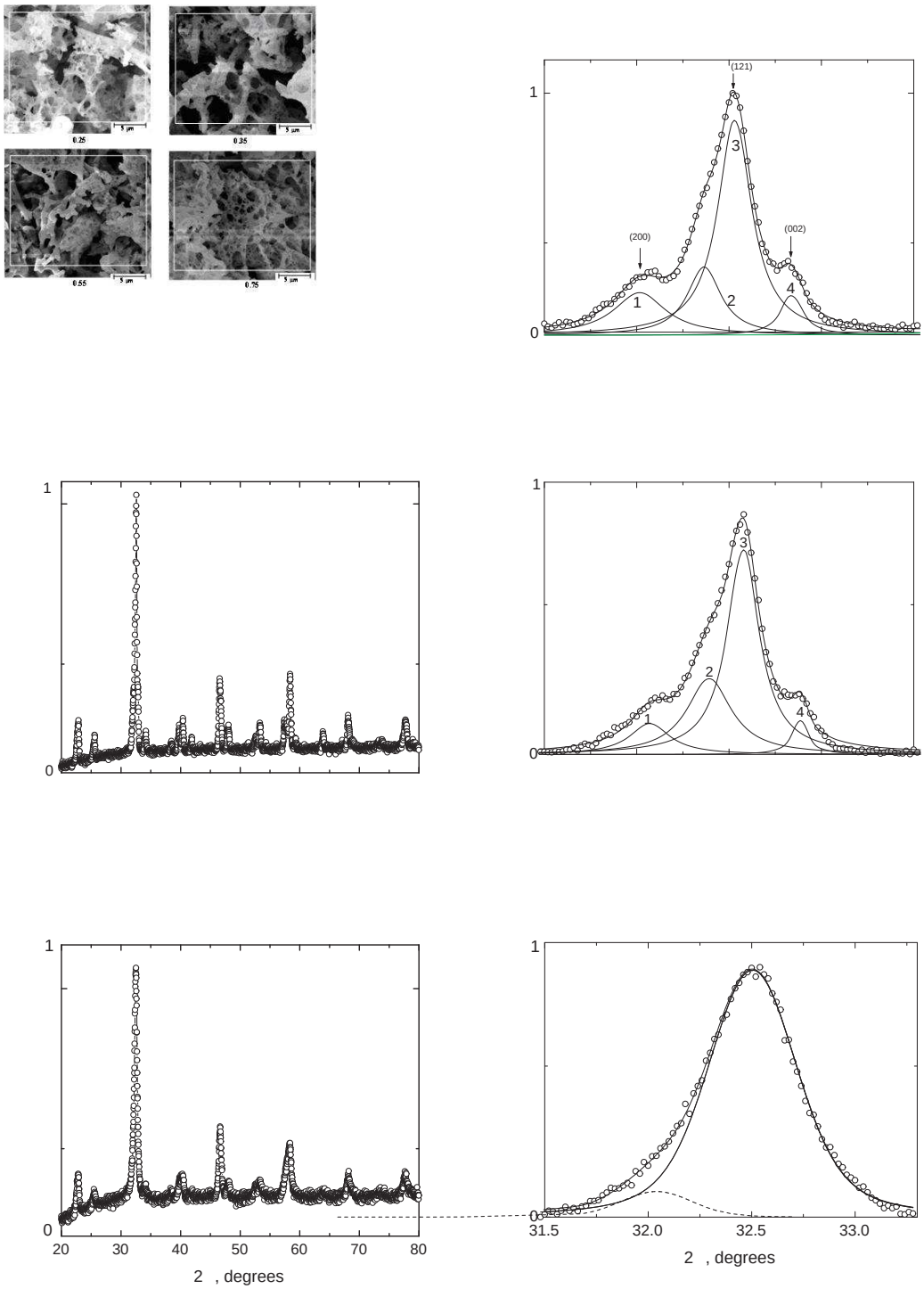
0.25
0.35
0.55
0.75
(121)
(200)
(002)
1
2
3
4
0
1
20
30
40
50
60
70
80
2 , degrees
31.5
32.0
32.5
33.0
2 , degrees

Fig. 2.

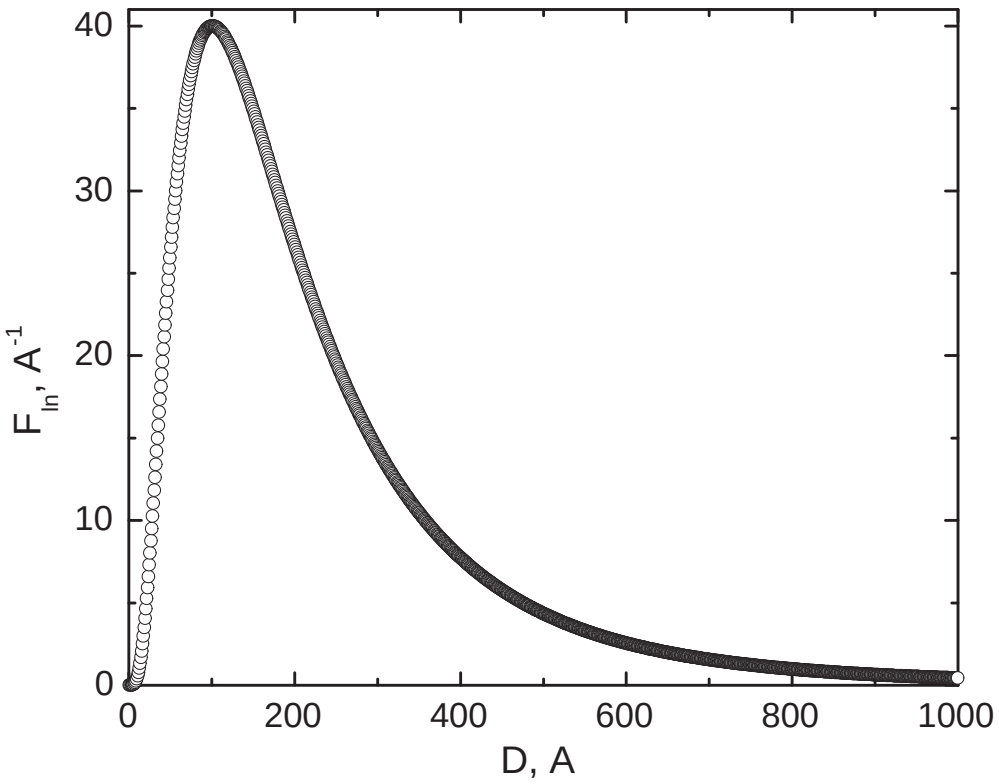

Fig. 3.